Moving Target Surrounding Control of Linear Multiagent Systems With Input Saturation

Bowen Xu, *Member, IEEE*, Hai-Tao Zhang, *Senior Member, IEEE*, Haofei Meng, Binbin Hu, Duxin Chen, *Member, IEEE*, and Guanrong Chen, *Life Fellow, IEEE*

***Abstract*—Formation control finds broad applications in numerous fields, such as cooperative detection, surveillance, transportation, and disaster rescue. In this article, aiming at hunting a moving target, a two-stage surrounding control algorithm is proposed for linear multiagent systems subject to input saturations. An adaptive distributed observer is developed for each agent to reconstruct the target's position. With the assistance of the algebraic graph theory and low gain feedback technique, distributed controllers are designed to drive the agents to encircle the moving target with a fixed radius and evenly distributed phase angles. Finally, both numerical simulations and experiments are conducted to verify the effectiveness of the proposed control algorithm.**

***Index Terms*—Distributed estimation, input saturation, multiagent systems (MASs), surrounding control.**

I. Introduction

RECENT years have witnessed a tremendous development of multiagent systems (MASs) control, due to its potential in various applications, such as autonomous unmanned vehicles [1], [2], robot [3], [4], biological systems [5], and smart grid [6]. The objective of MASs control is to accomplish some tasks in the network environment based on distributed sensing, interaction communication, and intelligent computing. In the past two decades, a great deal of efforts have been devoted to related tasks, such as consensus [7]–[9], synchronization [10]–[12], flocking [13]–[15], coordination [16]–[18], etc.

Formation control, which is one of the most actively studied topics regarding MASs, aims at generating a desired motion pattern or maintaining a formation with prescribed relative positions and orientations of the agents. In particular, surrounding formation control has attracted extensive attention from various research communities due to its wide applications in escorting, patrolling, rescuing, hunting, and detecting with multiple unmanned systems. In such a scenario, all the agents are driven to surround a single or multiple targets, which are either stationary or moving. Especially, surrounding with evenly distributed phase angles can maximize the overall coverage and hence is practically useful. Along this line of research, stationary target surrounding control has been investigated. As representative examples, Kim and Sugie [19] proposed a cyclic pursuit control strategy to execute a target-enclosing task, which was later generalized to MIMO agents in the three-dimensional (3-D) space [20]. Chen *et al.* [21] proposed a leader–follower framework for both unbalanced and balanced surrounding formations, where the follower group was propelled to surround a cluster of leaders. Lan *et al.* [22] assumed reachability and used an invariance analysis scheme to develop a hybrid control protocol, which yields a balanced surrounding formation around a fixed target. Zheng *et al.* [23] investigated the enclosing problem of multiple autonomous nonholonomic mobile robots using only local bearing measurements and verified the control methods with further experiments. Chen [24] studied a target-fencing problem, where a group of autonomous vehicles forms a convex hull to fence a target. Regarding the stationary target encirclement, all the agents will generate and then maintain a relative rigid formation with a steady ratio of tangential velocity over angular velocity. However, as for a moving target, the surrounding control problem will be more challenging since the surrounding configuration cannot be kept rigid all along. Hence, the control strategies solving the stationary target case cannot be directly applied to the moving target case. One essential issue is how to eliminate the conversion between the global and the local frames. Moreover, the estimate of the target's information will complicate the theoretical analysis as well. As representative works concerning moving target surrounding control, Guo *et al.* [25] studied the case with single-integral dynamical target, whereas Shi *et al.* [26] considered double-integral dynamical target

Manuscript received February 4, 2020; revised June 16, 2020 and August 18, 2020; accepted October 7, 2020. This work was supported in part by the National Natural Science Foundation of China under Grant U1713203, Grant 51721092, Grant 61751303, and Grant 51729501; in part by the Hong Kong Research Grants Council through GRF under Grant CityU11200317; in part by the Guangdong Innovative and Entrepreneurial Research Team Program under Grant 2014ZT05G304; and in part by the Program for Core Technology Tackling Key Problem. This article was recommended by Associate Editor Z. Li. *(Corresponding author: Hai-Tao Zhang.)*

Bowen Xu, Hai-Tao Zhang, Haofei Meng, and Binbin Hu are with the School of Artificial Intelligence and Automation, Huazhong University of Science and Technology, Wuhan 430074, China, also with the Key Laboratory of Image Processing and Intelligent Control, Huazhong University of Science and Technology, Wuhan 430074, China, and also with the State Key Laboratory of Digital Manufacturing Equipment and Technology, Huazhong University of Science and Technology, Wuhan 430074, China (e-mail: xubowenjason@163.com; zht@mail.hust.edu.cn; hfmeng@hust.edu.cn; hbb@hust.edu.cn).

Duxin Chen is with the School of Mathematics, Southeast University, Nanjing 211189, China (e-mail: chendx@seu.edu.cn).

Guanrong Chen is with the Department of Electrical Engineering, City University of Hong Kong, Hong Kong (e-mail: gchen@ee.cityu.edu.hk).

Color versions of one or more figures in this article are available at https://doi.org/10.1109/TSMC.2020.3030706.

Digital Object Identifier 10.1109/TSMC.2020.3030706

with an identical and static surrounding geometry. Then, a novel exploring matrix was proposed in [27] to describe the relationship between the agent and the target, which was thereafter used for the estimation of the target's state. Later on, other efforts were devoted to moving targets with partially known information. Sharma *et al.* [28] developed a sliding-mode controller to achieve a target-centered circular formation with a rigid structure. Lieberman *et al.* [29] proposed a control protocol to yield an escort formation with the assistance of the Morse potential function [30], which was then implemented on autonomous ground robots. Considering the control cost, Marasco *et al.* [31] and Iskandarani *et al.* [32] applied a model predictive control to solve the motional target encirclement problem. As more realistic studies, Sharghi *et al.* [33] proposed a surrounding control protocol for two-dimensional linear MASs, and Franchi *et al.* [34] proposed a novel 3-D target encirclement controller with interagent collision avoidance. More recently, to attain ultrafast hunting, finite-time surrounding control algorithms were developed in [35]–[37]. Besides the aforementioned theoretical studies, the experimental investigation of surrounding control methods on nonholonomic mobile robots or unmanned vehicles was considered in [38]–[41]. Specifically, it was shown in [38] that flexible multirobot formation yielded by affine transformation could be used for mobile robots to pass through narrow and irregular channels.

On the other hand, it is common that the agents encounter input saturations or constraints. To the best of our knowledge, most reported results for surrounding control of MASs assume that the inputs of all agents are constraint free. However, if the control input is limited, the anticipated performance of the closed-loop system will be downgraded, and in a severe situation, input saturation may cause loss of closed-loop stability [42]. As a result, the system will be divergent and incapable of accomplishing the desired task. Besides, input constraints will cause loss of target tracking in surrounding control. Therefore, it is an important mission to investigate this problem. Chen *et al.* [43] addressed the surrounding control problem for Euler–Lagrange systems with input constraints using the command filter method, where the target is stationary and the encircling geometry is static. Later, Zhang *et al.* [44] investigated the encircling control problem for single-integral systems with nonconvex input constraints.

Motivated by the above discussions, in this article, the surrounding control problem is considered for linear MASs with input saturation, where the target is moving with a time-varying velocity. As a distributed control method, it is assumed here that not necessarily all but at least one agent can access the target's information. An adaptive distributed observer is afterward designed for each agent to recover the state of the target, where the error between the real state and the estimated state converges to zero. With the assistance of the algebraic graph theory and low gain feedback technique, the balanced surrounding configuration is achieved.

Briefly, the contribution of this article is twofold: 1) a two-stage surrounding control algorithm is developed to fulfill the moving target encircling mission of linear MASs with input saturation and 2) the semiglobal synchronization of such MASs is achieved by using a low gain feedback technique.

The remainder of this article is organized as follows. Section II presents preliminaries and the formulation of the surrounding control problem for a moving target. Section III proposes a surrounding control algorithm along with a comprehensive theoretical analysis. Numerical simulation results and experimental performances with unmanned surface vessels (USVs) are shown in Sections IV and V, respectively, to verify the effectiveness of the proposed scheme. Finally, the conclusion is drawn in Section VI.

Throughout this article, the following notations will be used. $\mathbb{R}$ denotes the real space, N is the number of agents in MASs, I_n denotes the identity matrix of dimension n, $\|\cdot\|$ represents the Euclidean norm, and "$\otimes$" denotes the Kronecker product. A positive-definite matrix P is denoted as $P > 0$. The symbol $\mathbf{1}_n := [1, \dots, 1]^{\mathsf{T}}_{n\times 1}$.

II. Preliminaries and Problem Formulation

Let the network topology be represented by a fixed directed graph $\mathcal{G} = \{\mathcal{V}, \mathcal{E}, \mathcal{A}\}$, where $\mathcal{V} = \{1, 2, \dots, N\}$ is the node set, $\mathcal{E} \in \mathcal{V} \times \mathcal{V}$ is the edge set, and $\mathcal{A} = [a_{ij}] \in \mathbb{R}^{N\times N}$ is the weighted adjacency matrix. The edge in $\mathcal{G}$ is denoted by the ordered pair (i, j), and $(j, i) \in \mathcal{E}$ if and only if $a_{ij} \neq 0$. The set of neighbors of node i is denoted by $\mathcal{N}_i = \{j \in \mathcal{V} : (j, i) \in \mathcal{E}\}$. Only simple graph is considered, i.e., no self-loops are allowed in $\mathcal{G}$. The Laplacian $L = [l_{ij}] \in \mathbb{R}^{N\times N}$ associated with $\mathcal{G}$ is defined with $l_{ij} = \sum_{k=1,k\neq i}^{N} a_{ik}$ for $i = j$ and $l_{ij} = -a_{ij}$ for $i \neq j$. If the directed graph $\mathcal{G}$ contains a directed spanning tree, the Laplacian has a simple eigenvalue 0 with the corresponding eigenvector $\mathbf{1} = [1, 1, \dots, 1]^{\mathsf{T}}$, i.e., $L\mathbf{1} = 0$.

Consider an N-agent MAS with each agent $i \in \mathcal{V}$ subject to input saturation, whose dynamics is described by the following continuous-time linear model:

$$\begin{aligned} \dot{x}_i &= Ax_i + B\sigma(u_i) \\ y_i &= Cx_i,\ i \in \mathcal{V} \end{aligned} \tag{1}$$

where $x_i \in \mathbb{R}^n$ is the state of agent i, $y_i \in \mathbb{R}^2$ is the measurement output of agent i representing the position of the agent, $u_i \in \mathbb{R}^m$ is the control input, σ is a saturation function defined as $\sigma(u_i) = [\mathrm{sat}(u_{i1}), \mathrm{sat}(u_{i2}), \dots, \mathrm{sat}(u_{im})]^{\mathsf{T}}$, $\mathrm{sat}(u) = \mathrm{sign}(u)\min\{\Delta, |u|\}$ for constant $\Delta > 0$, $\mathrm{sign}(\cdot)$ is the signum function, and A, B, and C are constant matrices with appropriate dimension. The dynamics of the moving target is described by

$$\begin{aligned} \dot{r} &= Sr \\ y_r &= C_r r \end{aligned} \tag{2}$$

with $r \in \mathbb{R}^q$, $y_r \in \mathbb{R}^2$ representing the state and position of the target, respectively, and constant matrices S and C_r.

Problem 1: Consider an MAS governed by (1) and $\mathcal{G} = \{\mathcal{V}, \mathcal{E}, \mathcal{A}\}$, design a controller to drive all agents $i \in \mathcal{V}$ to encircle the moving target (2) (i.e., move along a common circle centered at the target) with a balanced (i.e., uniform) distribution (as Fig. 1). The problem is solved via two stages.

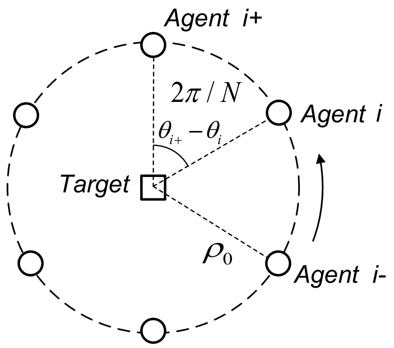

Fig. 1. Balanced surrounding configuration. The square denotes the moving target, whereas circles denote the agents. The prescribed surrounding radius is ρ_0, and the uniform phase difference is $2\pi/N$.

Stage 1: For any $\epsilon_i > 0$, there always exists a time $T > 0$ such that for $t \geq T$

$$\|y_i - y_r\| \leq \rho + \epsilon_i, t \geq T, \quad i \in \mathcal{V}. \tag{3}$$

Stage 2: All the agents encircle the target with a prescribed radius ρ_0 and evenly distributed phase angles, i.e.,

$$\lim_{t\to\infty} \|y_i - y_r\| = \rho_0$$
$$\lim_{t\to\infty} \left|\theta_{i+/i-} - \theta_i\right| = 2\pi/N, \quad i \in \mathcal{V} \tag{4}$$

where $\theta_{i+}(\theta_{i-})$ denote the phase angle of the forward (backward) neighbor of agent i.

Remark 1: It is assumed that if an agent is moving close to the target within its sensing range, it can access the information of the target. Stage 1 aims to drive all the agents $\mathcal{V}$ into a neighborhood of the target, where they are sufficiently close to the circle centered at the target with a radius ρ. Thus, the state of the target can be accessed by all the agents $\mathcal{V}$. Denote the sensing radius with respect to the target as $\rho^* = \rho + \epsilon^*$ for some $\epsilon^* \geq \max_{i\in\mathcal{V}} \epsilon_i$.

To address Problem 1, the following assumptions are made.

Assumption 1: The network topology $\mathcal{G}$ has a directed spanning tree.

Assumption 2: The pair (A, B) is asymptotically null controllable with bounded controls (ANCBC) [45], i.e., (A, B) is stabilizable and all the eigenvalues of A are located in the closed left-half s-plane. The pair (A, C) is detectable.

Define $g_i > 0$ if agent $i \in \mathcal{V}$ have access to the state information of the moving target and otherwise $g_i = 0$.

Assumption 3: During Stage 1 of Problem 1, there exists at least one agent $i \in \mathcal{V}$ such that $g_i > 0$.

Assumption 4: All the eigenvalues of S in (2) are simple and have zero real parts. Also, there exists $\varpi_r > 0$ such that

$$\|r(0)\| \leq \varpi_r. \tag{5}$$

Remark 2: Assumption 4 is made without loss of generality. In fact, if the surrounding control problem is solvable under Assumption 4, then it is also solvable when S is Hurwitz. However, due to the existence of input saturation, the surrounding control may not realize if S has some unstable modes.

Lemma 1 [46]: Let Assumption 2 hold. Then, for a constant $\beta > 0$ and each $\varepsilon \in (0, 1]$, there exists a unique symmetrical matrix $P(\varepsilon) > 0$ solving the parametric algebraic Riccati equation

$$A^{\mathsf{T}}P(\varepsilon) + P(\varepsilon)A - \beta P(\varepsilon)BB^{\mathsf{T}}P(\varepsilon) + \varepsilon I = 0 \tag{6}$$

with $\lim_{\varepsilon\to 0} P(\varepsilon) = 0$.

III. Main Results

A. Stage 1: Approaching the Neighborhood of the Target

Consider a group of agents moving in the circular motion with input saturation and construct a distributed controller to achieve balanced surrounding control explicitly. The MAS is given as follows:

$$\dot{x}_i = Ax_i + \sigma(u_i), i \in \mathcal{V} \tag{7}$$
$$\dot{r} = Sr \tag{8}$$

where $A = \begin{bmatrix} 0 & -\omega_0 \\ \omega_0 & 0 \end{bmatrix}$, ω_0 is a constant, and $x_i \in \mathbb{R}^2$ and $r \in \mathbb{R}^2$ represent the states of the agents and the target, respectively. Here, $y_i = x_i$ and $y_r = r$. $u_i \in \mathbb{R}^2$ is the controller to be designed. It is noticed that the system (7) is ANCBC. Define the error between an agent and the target as

$$\xi_i = x_i - r \tag{9}$$

whose derivative is

$$\dot{\xi}_i = \dot{x}_i - \dot{r} = A\xi_i + \sigma(u_i) + (A - S)r. \tag{10}$$

To illustrate the convergence of ξ_i, a lemma is needed.

Lemma 2: If there exists ξ_0 governed by

$$\dot{\xi}_0 = A\xi_0 \tag{11}$$

such that

$$\lim_{t\to\infty} (\xi_i - \xi_0) = 0$$

then

$$\lim_{t\to\infty} \|x_i - r\| = \rho.$$

Proof: With the dynamics (11) and the form of A, the solution of (11) can be presented as $\xi_0(t) = \begin{bmatrix} \rho\cos(\omega_0 t + \varphi_0) \\ \rho\sin(\omega_0 t + \varphi_0) \end{bmatrix}$ with $\rho > 0$ and $\varphi_0 > 0$. It follows that:

$$\|\xi_0(t)\| = \left\| \begin{bmatrix} \rho\cos(\omega_0 t + \varphi_0) \\ \rho\sin(\omega_0 t + \varphi_0) \end{bmatrix} \right\| = \rho.$$

Thus

$$\lim_{t\to\infty} \|x_i - r\| = \lim_{t\to\infty} \|\xi_i\| = \|\xi_0\| = \rho.$$

■

Based on Assumption 3, to preserve the decentralized nature of the controller, an adaptive distributed observer $\widehat{r}_i$ is designed similar to [47] for each agent as follows:

$$\dot{\widehat{r}}_i = S\widehat{r}_i + \sum_{j\in\mathcal{N}_i} a_{ij}C_r\left(\widehat{r}_i - \widehat{r}_j\right) + g_i C_r\left(\widehat{r}_i - r\right) \tag{12}$$

where $\|\widehat{r}(0)\| \leq \widehat{\varpi}_r$, $\widehat{r}(0) = [\widehat{r}_1^{\mathsf{T}}(0), \widehat{r}_2^{\mathsf{T}}(0), \ldots, \widehat{r}_N^{\mathsf{T}}(0)]^{\mathsf{T}}$, and C_r is the observer matrix. To design the distributed observer, the following lemma will be needed.

Lemma 3: If $S+\overline{\lambda}_i C_r$, $i=1,\ldots,N$, is Hurwitz, then

$$\lim_{t\to\infty}\widehat{r}_i = r,\ \ i=1,\ldots,N$$

which can be implemented, where $\overline{\lambda}_i$ is the ith eigenvalue of matrix $L+G$, $G=\mathrm{diag}\{g_1,g_2,\ldots,g_N\}$.

Proof: Define the errors $e_{r_i}=\widehat{r}_i - r$. Then

$$\begin{aligned}\dot{e}_{r_i} &= \dot{\widehat{r}}_i - \dot{r}\\ &= Se_{r_i} + \sum_{j\in\mathcal{N}_i} a_{ij}C_r\big(e_{r_i}-e_{r_j}\big) + g_iC_re_{r_i}.\end{aligned} \tag{13}$$

Rewrite (13) in a compact form as

$$\dot{e}_r = (I_N\otimes S + (L+G)\otimes C_r)e_r \tag{14}$$

with $e_r=[e_{r_1}^{\mathsf T}, e_{r_2}^{\mathsf T},\ldots,e_{r_N}^{\mathsf T}]^{\mathsf T}$. Consider a Lyapunov function

$$V(e_r) = e_r^{\mathsf T}P_Re_r \tag{15}$$

where $P_R = I_N\otimes P_r$, with P_r being a symmetrical positive-definite matrix. According to [48, Th. 1], if $S+\overline{\lambda}_iC_r$ is Hurwitz, then $\dot{V}(e_r) = -e_r^{\mathsf T}Q_Re_r$ with $Q_R = -(I_N\otimes(S^{\mathsf T}P_r+P_rS) + (L+G)^{\mathsf T}\otimes C_r^{\mathsf T}P_r + (L+G)\otimes P_rC_r)$, which implies that $\lim_{t\to\infty} e_r = 0$, i.e., $\lim_{t\to\infty}\widehat{r}_i = r$, completing the proof. ■

Remark 3: From (15), one has

$$\|e_r\|^2 \le \frac{\lambda_{\max}(P_R)}{\lambda_{\min}(P_R)}\|e_r(0)\|^2 = \lambda^*\|e_r(0)\|^2.$$

Moreover, $e_r(0) = \widehat{r}(0) - \mathbf{1}_Nr(0)$ and $\|e_r(0)\| \le \|\widehat{r}(0)\| + \|\mathbf{1}_Nr(0)\|$, which shows that e_r is bounded.

Next, based on the low gain feedback technique proposed in [46], design a control law for (10) as

$$u_i = -P(\varepsilon)\sum_{j\in\mathcal{N}_i}a_{ij}\big(x_i-x_j\big) - T_r\widehat{r}_i \tag{16}$$

where $P(\varepsilon)$ is obtained by (6) and T_r is a feedback matrix. The closed-loop system is

$$\dot{x}_i = Ax_i + \sigma\left[-P(\varepsilon)\sum_{j\in\mathcal{N}_i}a_{ij}\big(x_i-x_j\big) - T_r\widehat{r}_i\right]. \tag{17}$$

If $\|u_i\|\le\Delta$, then let $T_r = A-S$. It follows from (10) and (16) that:

$$\dot{\xi}_i = A\xi_i - P(\varepsilon)\sum_{j\in\mathcal{N}_i}a_{ij}\big(\xi_i-\xi_j\big) - (A-S)e_{r_i}$$

which can be rewritten in a compact form as

$$\dot{\xi} = [I_N\otimes A - L\otimes P(\varepsilon)]\xi - [I_N\otimes(A-S)]e_r \tag{18}$$

where $\xi = [\xi_1^{\mathsf T},\xi_2^{\mathsf T},\ldots,\xi_N^{\mathsf T}]^{\mathsf T}$. Conduct a coordinate transformation for ξ as

$$\xi = \overline{T}_\xi\overline{\xi},\quad \overline{T}_\xi = T_\xi\otimes I_l \tag{19}$$

with $\xi_i\in\mathbb{R}^l$, $i=1,2,\ldots,N$, satisfying

$$T_\xi = \begin{bmatrix}\mathbf{1}_N & Y\end{bmatrix},\ T_\xi^{-1} = \begin{bmatrix} r^{\mathsf T}\\ W\end{bmatrix}$$

and $r^{\mathsf T} = [r_1,\ldots,r_N]$ is the left eigenvector of the Laplacian associated with the zero eigenvalue. Substituting (19) to (18) yields

$$\overline{T}_\xi\dot{\overline{\xi}} = [I_N\otimes A - L\otimes P(\varepsilon)]\overline{T}_\xi\overline{\xi} - [I_N\otimes(A-S)]e_r.$$

Thus, one has

$$\begin{aligned}\dot{\overline{\xi}} &= \Big(T_\xi^{-1}\otimes I_l\Big)(I_N\otimes A - L\otimes P(\varepsilon))\big(T_\xi\otimes I_l\big)\overline{\xi}\\ &\quad - \Big(T_\xi^{-1}\otimes I_l\Big)(I_N\otimes(A-S))e_r\\ &= (I_N\otimes A)\overline{\xi} - \Big(T_\xi^{-1}LT_\xi\otimes P(\varepsilon)\Big)\overline{\xi} - \Big(T_\xi^{-1}\otimes(A-S)\Big)e_r\\ &= (I_N\otimes A)\overline{\xi} - \left(\begin{bmatrix}0 & 0\\ 0 & J\end{bmatrix}\otimes P(\varepsilon)\right)\overline{\xi} - \Big(T_\xi^{-1}\otimes(A-S)\Big)e_r\end{aligned}$$

where the diagonal entries of J are the nonzero eigenvalues of L. Partitioning $\overline{\xi}$ as $\overline{\xi} = [\overline{\xi}_1,\overline{\xi}_2]^{\mathsf T}$, and denoting $\overline{\xi}_1 = (r^{\mathsf T}\otimes I_l)\xi$, $\overline{\xi}_2 = (W\otimes I_l)\xi$ with coordinate transformation (19), one has

$$\begin{cases}\dot{\overline{\xi}}_1 = A\overline{\xi}_1 + B_1e_r\\ \dot{\overline{\xi}}_2 = (I_{N-1}\otimes A - J\otimes P(\varepsilon))\overline{\xi}_2 + B_2e_r.\end{cases} \tag{20}$$

To derive the main technical result, the following lemma is needed.

Lemma 4: If $\|u_i\|\le\Delta$, and $\lim_{t\to\infty}\mathrm{col}\{e_r(t),\overline{\xi}_2(t)\} = 0$ exponentially, then

$$\lim_{t\to\infty}(\xi_i - \xi_0) = 0.$$

Proof: Analogously to the proof of [49, Corollary 4.1], let ξ_0 be a trajectory governed by (11) with the initial value $\xi_0(0)$ to be determined. Define $\widetilde{\xi} := \overline{\xi}_1 - \xi_0$. Then, the state $\widetilde{\xi}$ is governed by

$$\dot{\widetilde{\xi}} = A\widetilde{\xi} + B_1e_r$$

and its solution is obtained as follows:

$$\begin{aligned}\widetilde{\xi}(t) &= e^{At}\widetilde{\xi}(0) + \int_0^t e^{A(t-\tau)}B_1e^{A_e\tau}e_r(0)d\tau\\ &= e^{At}\big[\widetilde{\xi}(0) + s(t)\big]\end{aligned}$$

with

$$s(t) = \int_0^t e^{-A\tau}B_1e^{A_e\tau}e_r(0)d\tau.$$

Since all the eigenvalues of A are on the image axis and A_e is Hurwitz by Lemma 3, the limit $s_\infty = \lim_{t\to\infty}s(t)$ exists and is finite. Now choose the initial value for $\xi_0(t)$ as follows:

$$\xi_0(0) = \overline{\xi}_1(0) + s_\infty.$$

Then

$$\lim_{t\to\infty}\big[\widetilde{\xi}(0) + s(t)\big] = \overline{\xi}_1(0) - \xi_0(0) + s_\infty = 0$$

which implies that $\lim_{t\to\infty}\widetilde{\xi}(t) = 0$, i.e., $\lim_{t\to\infty}[\overline{\xi}_1(t) - \xi_0(t)] = 0$. Moreover, since $\overline{\xi}_2$ is asymptotically stable, it follows from (19) that:

$$\lim_{t\to\infty}\xi = \big(\begin{bmatrix}\mathbf{1}_N & Y\end{bmatrix}\otimes I_l\big)\begin{bmatrix}\overline{\xi}_1\\ \overline{\xi}_2\end{bmatrix} = [\mathbf{1}_N\otimes I_l]\overline{\xi}_1$$

which immediately leads to $\lim_{t\to\infty}\xi_i = \overline{\xi}_1$. Thereby, one has $\lim_{t\to\infty}\xi_i = \xi_0$. ■

Theorem 1: Consider an N-agent MAS governed by (7) and $\mathcal{G} = \{\mathcal{V},\mathcal{E},\mathcal{A}\}$ with a moving target (8). Suppose that Assumptions 1, 3, and 4 hold, with *a priori* given bounded set

$\Omega(x) \subset \mathbb{R}^2$. Construct the control input u_i as given by (16). Then, one has

$$\lim_{t\to\infty}\|x_i - r\| = \rho$$

provided that $x_i(0) \in \Omega(x)$, $i \in \mathcal{V}$, $\|r(0)\| \le \varpi_r$, $\|\widehat{r}(0)\| \le \widehat{\varpi}_r$.

Proof: Since $\xi_i - \xi_j = x_i - x_j$ by (9), the control input u_i can be rewritten as

$$u_i = -(L_i \otimes P(\varepsilon))\xi - (A - S)\widehat{r}_i \tag{21}$$

where L_i is the ith row of the Laplacian matrix. With the transformation (19), it follows that:

$$\begin{aligned} u_i &= -(L_i \otimes P(\varepsilon))([\mathbf{1}_N \quad Y] \otimes I_l)\overline{\xi} - (A - S)\widehat{r}_i \\ &= -([L_i\mathbf{1}_N \quad L_iY] \otimes P(\varepsilon))\overline{\xi} - (A - S)\widehat{r}_i \\ &= -([0 \quad L_iY] \otimes P(\varepsilon))\begin{bmatrix}\overline{\xi}_1 \\ \overline{\xi}_2\end{bmatrix} - (A - S)\widehat{r}_i \\ &= -(L_iY \otimes P(\varepsilon))\overline{\xi}_2 - (A - S)\widehat{r}_i. \end{aligned} \tag{22}$$

Consider a Lyapunov function

$$V(\overline{\xi}_2) = \overline{\xi}_2^{\mathsf{T}}T(\varepsilon)\overline{\xi}_2 \tag{23}$$

with $T(\varepsilon) = I_{N-1} \otimes P(\varepsilon)$. Let $m_\xi > 0$ be a constant satisfying

$$\sup_{\varepsilon\in(0,1],x_i(0)\in\Omega(x)} \overline{\xi}_2^{\mathsf{T}}(0)T(\varepsilon)\overline{\xi}_2(0) \le m_\xi.$$

It is noted that r is bounded, $\overline{\xi}_2(0) = (W \otimes I_l)(x(0) - \mathbf{1}_N r(0))$ is bounded as well provided $x_i(0) \in \Omega(x)$. Thus, such an m_ξ exists since $\Omega(x)$ is bounded and $\lim_{\varepsilon\to0}P(\varepsilon) = 0$ by Lemma 1. Define a level set $L_V(m_\xi) := \{\overline{\xi}_2 \in \mathbb{R}^{(N-1)l} : V(\overline{\xi}_2) \le m_\xi\}$. Then, $\overline{\xi}_2 \in L_V(m_\xi)$ implies that

$$\left\|P(\varepsilon)\sum_{j\in\mathcal{N}_i} a_{ij}\left(x_i - x_j\right)\right\| \le \delta_1$$

and

$$\begin{aligned} \|\widehat{r}_i\| &\le \left\|e_{r_i}\right\| + \|r\| \le \|e_r\| + \|r\| \le \sqrt{\lambda^*}\|e_r(0)\| + \|r\| \\ &\le \sqrt{\lambda^*}(\|\widehat{r}(0)\| + \|\mathbf{1}_N r(0)\|) + \|r\| \le \frac{\Delta - \delta_1}{\|A - S\|} \end{aligned}$$

where $\widehat{\varpi}_r = [[(\Delta - \delta_1)/(\|A - S\|)] - (\sqrt{N\lambda^*} + \kappa_s)\varpi_r]/\sqrt{\lambda^*}$ with fixed $\kappa_s = \|e^{St}\|$. Therefore

$$\|u_i\| \le \left\|P(\varepsilon)\sum_{j\in\mathcal{N}_i} a_{ij}(t)\left(x_i - x_j\right)\right\| + \|(A - S)\widehat{r}_i\| \le \Delta. \tag{24}$$

Next, it is to prove that $\overline{\xi}_2$ is asymptotically stable. Let $A_\xi := I_{N-1} \otimes A - J \otimes P(\varepsilon)$. Then, the derivative of $V(\overline{\xi}_2)$ is

$$\begin{aligned} \dot{V}(\overline{\xi}_2) &= \dot{\overline{\xi}}_2^{\mathsf{T}}T(\varepsilon)\overline{\xi}_2 + \overline{\xi}_2^{\mathsf{T}}T(\varepsilon)\dot{\overline{\xi}}_2 \\ &= \left(A_\xi\overline{\xi}_2 + B_2e_r\right)^{\mathsf{T}}T(\varepsilon)\overline{\xi}_2 + \overline{\xi}_2^{\mathsf{T}}T(\varepsilon)\left(A_\xi\overline{\xi}_2 + B_2e_r\right) \\ &= \overline{\xi}_2^{\mathsf{T}}\left[A_\xi^{\mathsf{T}}T(\varepsilon) + T(\varepsilon)A_\xi\right]\overline{\xi}_2 + 2\overline{\xi}_2^{\mathsf{T}}T(\varepsilon)B_2e_r. \end{aligned} \tag{25}$$

Therein

$$\begin{aligned} A_\xi^{\mathsf{T}}T(\varepsilon) + T(\varepsilon)A_\xi &= I_{N-1} \otimes \left(A_\xi^{\mathsf{T}}P(\varepsilon) + P(\varepsilon)A_\xi\right) \\ &\quad - (J^{\mathsf{T}} + J) \otimes P(\varepsilon)P(\varepsilon). \end{aligned}$$

Due to the symmetry of $J^{\mathsf{T}} + J$, there always exists an orthogonal matrix T_J such that

$$J^{\mathsf{T}} + J = T_J^{\mathsf{T}}\mathrm{diag}\left\{\lambda_1(J^{\mathsf{T}} + J)\lambda_2(J^{\mathsf{T}} + J)\cdots\lambda_{N-1}(J^{\mathsf{T}} + J)\right\}T_J.$$

Letting $\widetilde{\xi}_2 = (T_J \otimes I_l)\overline{\xi}_2$, with Lemma 1, it follows that:

$$\begin{aligned} \overline{\xi}_2^{\mathsf{T}}\left[A_\xi^{\mathsf{T}}T(\varepsilon) + T(\varepsilon)A_\xi\right]\overline{\xi}_2 &\le \widetilde{\xi}_2^{\mathsf{T}}\Big(A_\xi^{\mathsf{T}}P(\varepsilon) + P(\varepsilon)A_\xi \\ &\qquad - \beta P(\varepsilon)P(\varepsilon)\Big)\widetilde{\xi}_2 \\ &= -\varepsilon\overline{\xi}_2^{\mathsf{T}}\left(T_J^{\mathsf{T}} \otimes I_l\right)(T_J \otimes I_l)\overline{\xi}_2 \end{aligned}$$

with $\beta \le \min\{\lambda(J^{\mathsf{T}} + J)\}$ and therefore $A_\xi^{\mathsf{T}}T(\varepsilon) + T(\varepsilon)A_\xi$ can be denoted as $-Q_\xi$ with $Q_\xi > 0$. Moreover

$$2\overline{\xi}_2^{\mathsf{T}}T(\varepsilon)B_2e_r \le \frac{1}{\eta}\overline{\xi}_2^{\mathsf{T}}T(\varepsilon)B_2B_2^{\mathsf{T}}T(\varepsilon)\overline{\xi}_2 + \eta e_r^{\mathsf{T}}e_r$$

where η is a positive constant. Thus

$$\begin{aligned} \dot{V}(\overline{\xi}_2) &\le -\varepsilon\overline{\xi}_2^{\mathsf{T}}\left(T_J^{\mathsf{T}} \otimes I_l\right)(T_J \otimes I_l)\overline{\xi}_2 + \frac{1}{\eta}\overline{\xi}_2^{\mathsf{T}}T(\varepsilon)B_2B_2^{\mathsf{T}}T(\varepsilon)\overline{\xi}_2 \\ &\quad + \eta e_r^{\mathsf{T}}e_r \\ &\le -\frac{\eta\kappa_e^2}{m_\xi}\overline{\xi}_2^{\mathsf{T}}(I_{N-1} \otimes P(\varepsilon))\overline{\xi}_2 + \eta\kappa_e^2 \end{aligned} \tag{26}$$

with $\kappa_e = \sqrt{\lambda^*}\widehat{\varpi}_r + \sqrt{N\lambda^*}\varpi_r$. Observing that on the boundary of $L_V(m_\xi)$, $\dot{V}(\overline{\xi}_2) \le 0$, which indicates that $L_V(m_\xi)$ is an invariant set for each $\overline{\xi}_2 \in L_V(m_\xi)$ and $\lim_{t\to\infty}\overline{\xi}_2 = 0$ with the exponential stability of e_r. By Lemmas 2 and 4, one has

$$\lim_{t\to\infty}\|x_i - r\| = \lim_{t\to\infty}\|\xi_i\| = \lim_{t\to\infty}\|\xi_0\| = \rho$$

which completes the proof. ∎

Remark 4: It follows from Assumption 4 that all the eigenvalues of S are simple with zero real parts. Let $S = UJU^{-1}$ and $J = \begin{bmatrix} s_1j & 0 \\ 0 & s_2j\end{bmatrix}$ with s_1j and s_2j being the eigenvalues of S, and j the imaginary unit. One thus has

$$\begin{aligned} \left\|e^{St}\right\| &= \left\|Ue^{Jt}U^{-1}\right\| \le \|U\| \cdot \left\|\begin{bmatrix} e^{s_1jt} & 0 \\ 0 & e^{s_2jt}\end{bmatrix}\right\| \cdot \left\|U^{-1}\right\| \\ &= \|U\| \cdot \left\|U^{-1}\right\| = \kappa_s \end{aligned}$$

which implies that κ_s is fixed.

Remark 5: From Theorem 1, it is easy to see that for any ϵ_i, there exists $T > 0$ such that (3) holds. To solve Problem 1 following the two stages, one needs to explicitly establish the relationship between ϵ_i and T such that the switching between the two stages can be controlled. The following corollary presents the relationship.

Corollary 1: Consider a MAS of N agents governed by (7) and $\mathcal{G} = \{\mathcal{V}, \mathcal{E}, \mathcal{A}\}$ with a moving target (8). Suppose that Assumptions 1, 3, and 4 hold, with *a priori* given bounded set $\Omega(x) \subset \mathbb{R}^2$. Construct the control input u_i as given by (16). Then, Stage 1 of Problem 1 is solvable, where ϵ_i and T satisfy

$$\varsigma_i\sqrt{\frac{e^{-\alpha^*T}\left(\xi^{\mathsf{T}}(0)\left(W^{\mathsf{T}}W \otimes P(\varepsilon)\right)\xi(0)\right) + \beta_\xi T)}{\lambda_{\min}(T(\varepsilon))}} \le \epsilon_i$$

with ς_i is the norm of the ith row of Y, $\alpha^* = \min\{|\alpha_\xi|, |\alpha_r|\}$, $\alpha_\xi = [(-\lambda_{\min}(Q_\xi) + (1/\zeta)\|T(\varepsilon)B_2\|)/(\lambda_{\min}(T(\varepsilon)))] < 0$

with constant $\zeta > 0$, $\alpha_r = [(\lambda_{\min}(Q_R))/(\lambda_{\min}(P_R))]$, $\beta_\xi = [(4\zeta\|T(\varepsilon)B_2\|e_r^{\top}(0)P_R e_r(0))/(\lambda_{\min}(P_R))]$.

Proof: Consider the Lyapunov function (15). One can obtain the following inequality:

$$\lambda_{\min}(P_R)\|e_r\|^2 \le V(e_r) \le \lambda_{\max}(P_R)\|e_r\|^2. \tag{27}$$

Meanwhile, from Lemma 3, one can acquire

$$\dot{V}(e_r) \le -\lambda_{\min}(Q_R)\|e_r\|^2. \tag{28}$$

Substitute (27) into (28) yields the Gronwall inequality

$$\dot{V}(e_r) \le -\frac{\lambda_{\min}(Q_R)}{\lambda_{\min}(P_R)}V(e_r). \tag{29}$$

Let $\alpha_r = [(\lambda_{\min}(Q_R))/(\lambda_{\min}(P_R))] > 0$. Then, (29) is solved yielding

$$V(e_r) \le e^{-\alpha_r t}V(e_r(0)) \tag{30}$$

which immediately leads to

$$\|e_r\| \le \sqrt{\frac{e^{-\alpha_r t}V(e_r(0))}{\lambda_{\min}(P_R)}}. \tag{31}$$

From Theorem 1, $L_V(m_\xi)$ is an invariant set, and in $L_V(m_\xi)$, $\|u_i\| \le \Delta$ for all time. Based on the decomposition of $\bar{\xi}$ in (20), one has $\dot{\bar{\xi}}_2 = A_\xi\bar{\xi}_2 + B_2 e_r$, with $A_\xi = I_{N-1}\otimes A - J\otimes P(\varepsilon)$. Consider the Lyapunov function (23), one has the following inequality:

$$\lambda_{\min}(T(\varepsilon))\left\|\bar{\xi}_2\right\|^2 \le V\left(\bar{\xi}_2\right) \le \lambda_{\max}(T(\varepsilon))\left\|\bar{\xi}_2\right\|^2. \tag{32}$$

Meanwhile, it follows that:

$$\begin{aligned}\dot{V}\left(\bar{\xi}_2\right) &\le -\lambda_{\min}\left(Q_\xi\right)\left\|\bar{\xi}_2\right\|^2 + 2\left\|\bar{\xi}_2\right\|\|T(\varepsilon)B_2\|\|e_r\| \\ &\le -\lambda_{\min}\left(Q_\xi\right)\left\|\bar{\xi}_2\right\|^2 \\ &\quad + 2\|T(\varepsilon)B_2\|\left(\frac{1}{2\zeta}\left\|\bar{\xi}_2\right\|^2 + 2\zeta\|e_r\|^2\right) \\ &\le \left(-\lambda_{\min}\left(Q_\xi\right) + \frac{1}{\zeta}\|T(\varepsilon)B_2\|\right)\left\|\bar{\xi}_2\right\|^2 \\ &\quad + 4\zeta\|T(\varepsilon)B_2\|\|e_r\|^2 \end{aligned} \tag{33}$$

with $\zeta > 0$. Consider (31) and (32), one has

$$\begin{aligned}\dot{V}\left(\bar{\xi}_2\right) &\le \left(-\lambda_{\min}\left(Q_\xi\right) + \frac{1}{\zeta}\|T(\varepsilon)B_2\|\right)\frac{V\left(\bar{\xi}_2\right)}{\lambda_{\min}(T(\varepsilon))} \\ &\quad + 4\zeta\|T(\varepsilon)B_2\|\frac{e^{-\alpha_r t}V(e_r(0))}{\lambda_{\min}(P_R)}. \end{aligned} \tag{34}$$

Denote

$$\alpha_\xi = \frac{-\lambda_{\min}\left(Q_\xi\right) + \frac{1}{\zeta}\|T(\varepsilon)B_2\|}{\lambda_{\min}(T(\varepsilon))}$$
$$\beta_\xi = \frac{4\zeta\|T(\varepsilon)B_2\|e_r^{\top}(0)P_R e_r(0)}{\lambda_{\min}(P_R)}$$

it follows from (34) that:

$$\dot{V}\left(\bar{\xi}_2\right) \le \alpha_\xi V\left(\bar{\xi}_2\right) + \beta_\xi e^{-\alpha_r t}. \tag{35}$$

With an appropriately chosen ζ, one can make α_ξ negative. Denote $\alpha^* = \min\{|\alpha_\xi|, |\alpha_r|\}$. One has

$$\dot{V}\left(\bar{\xi}_2\right) \le -\alpha^* V\left(\bar{\xi}_2\right) + \beta_\xi e^{-\alpha^* t}.$$

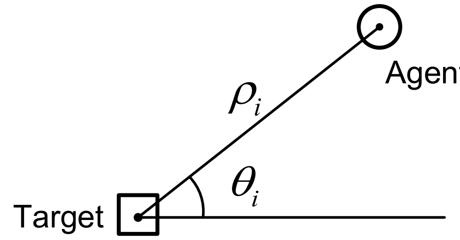

Fig. 2. Polar coordinates illustration. Here, the square and the circle denote the target and an agent, respectively. ρ_i and θ_i are the polar radius and the phase, respectively.

Moreover, according to the comparison principle and considering (32), one has

$$V\left(\bar{\xi}_2\right) \le e^{-\alpha^* t}\left(V\left(\bar{\xi}_2(0)\right) + \beta_\xi t\right) \tag{36}$$

and

$$\left\|\bar{\xi}_2\right\|^2 \le \frac{e^{-\alpha^* t}\left(V\left(\bar{\xi}_2(0)\right) + \beta_\xi t\right)}{\lambda_{\min}(T(\varepsilon))}. \tag{37}$$

Thus, for any $\bar{\delta} > 0$, there always exists some $T > 0$ such that, for any $t \ge T$

$$\left\|\bar{\xi}_2\right\| \le \sqrt{\frac{e^{-\alpha^* t}\left(V\left(\bar{\xi}_2(0)\right) + \beta_\xi t\right)}{\lambda_{\min}(T(\varepsilon))}} \le \bar{\delta}. \tag{38}$$

Recall that $\xi = (\mathbf{1}\otimes I_l)\bar{\xi}_1 + (Y\otimes I_l)\bar{\xi}_2$. One has $\xi_i = \bar{\xi}_1 + (Y_i\otimes I_l)\bar{\xi}_2$, with Y_i being the ith row of Y. Then, it follows from (38) that:

$$\begin{aligned}\|x_i - r\| = \|\xi_i\| \le \left\|\bar{\xi}_1\right\| + \varsigma_i\left\|\bar{\xi}_2\right\| \le \left\|\bar{\xi}_1\right\| + \varsigma_i\bar{\delta} \\ \le \rho + \varsigma_i\bar{\delta}, t \ge T.\end{aligned}$$

Thus, for any $\epsilon_i = \varsigma_i\bar{\delta}$, one has $\|x_i - r\| \le \rho + \epsilon_i$, $t \ge T$, which shows that Stage 1 is solved. ■

B. Stage 2: Even Phase Distribution

Based on Stage 1, for $t = T$, (3) is satisfied. Hence, for $t \ge T$, all the agents can sense the target. Denote T as the launching time of the phase distribution stage, and consider the phase distribution problem in the polar coordinates as shown in Fig. 2. Therein, the target is the pole, ρ_i is the polar radius, and θ_i is the phase. Thus, the coordinates relationship can be described as

$$x_i - r = \rho_i\begin{bmatrix}\cos\theta_i \\ \sin\theta_i\end{bmatrix} = \rho_i\angle\theta_i. \tag{39}$$

The initial phase distribution of the MAS in this stage is given by $\Omega(\theta)$. Now, design the control law for balanced phase distribution as

$$\bar{u}_i = R(\rho_i,\theta_i)\begin{bmatrix}-\varepsilon^*(\rho_i - \rho_0) \\ \varepsilon^*\delta\theta_i + \varepsilon^*\eta_\theta\end{bmatrix} + Sr - Ax_i \tag{40}$$

where

$$R(\rho_i,\theta_i) = \begin{bmatrix}\cos\theta_i & -\rho_i\sin\theta_i \\ \sin\theta_i & \rho_i\cos\theta_i\end{bmatrix}$$

ρ_0 is the desired surrounding radius, $0 < \varepsilon^* < 1$, $\eta_\theta > 0$ is a designed parameter, and

$$\begin{cases} \delta\theta_i := \theta_{i+1} - \theta_i, \;\; i = 1, \dots, N-1 \\ \delta\theta_N := \theta_1 - \theta_N + 2\pi, \;\; i = N. \end{cases}$$

Hence, the closed-loop system is

$$\begin{aligned} \dot{x}_i &= Ax_i + \sigma(\overline{u}_i) \\ &= Ax_i + \sigma\left\{ R(\rho_i, \theta_i) \begin{bmatrix} -\varepsilon^*(\rho_i - \rho_0) \\ \varepsilon^*\delta\theta_i + \varepsilon^*\eta_\theta \end{bmatrix} + Sr - Ax_i \right\}. \end{aligned}$$

Moreover, if $\|\overline{u}_i\| \le \Delta$, then the polar system can be denoted in the form of

$$\begin{cases} \dot{\rho}_i := u_{\rho_i} = -\varepsilon^*(\rho_i - \rho_0) \\ \dot{\theta}_i := u_{\theta_i} = \varepsilon^*\delta\theta_i + \varepsilon^*\eta_\theta. \end{cases} \tag{41}$$

Theorem 2: Consider an N-agent MAS (7). When Stage 1 of Problem 1 is solved, with the control law (40), if $x_i(0) \in \Omega(x)$ and $\theta_i(T) \in \Omega(\theta)$ for all $i \in \mathcal{V}$, Stage 2 of Problem 1 is solvable.

Proof: Define the difference of radii as $e_{\rho_i} := \rho_i - \rho_0$. Consider a Lyapunov function $V(e_{\rho_i}) = \sum_{i=1}^N \varepsilon^* e_{\rho_i}^2$. Let $m_\rho > 0$ be a constant such that

$$\sup_{\varepsilon^* \in (0,1], x_i(0) \in \Omega(x)} \sum_{i=1}^N \varepsilon^* e_{\rho_i}^2(T) \le m_\rho.$$

It is noted that, for $x_i(0) \in \Omega(x)$, $x_i(T)$ is bounded and $e_{\rho_i}(T) = \rho_i(T) - \rho_0 = x_i(T) - r(T) - \rho_0$ is bounded as well.

Next, define the phase disagreement as

$$\begin{aligned} e_{\theta_i} &= \theta_{i+1} - \theta_i - 2\pi/N = \delta\theta_i - 2\pi/N, \;\; i = 1, \dots, N-1 \\ e_{\theta_N} &= \theta_1 - \theta_N + 2\pi - 2\pi/N = \delta\theta_N - 2\pi/N, \;\; i = N. \end{aligned}$$

Consider the Lyapunov function $V(e_\theta) = \sum_{i=1}^N \varepsilon^* e_{\theta_i}^2$, and let $m_\theta > 0$ ba a constant such that

$$\sup_{\varepsilon^* \in (0,1], e_{\theta_i}(T) \in \Omega(e_\theta)} \sum_{i=1}^N \varepsilon^* e_{\theta_i}^2(T) \le m_\theta$$

where $\Omega(e_\theta) := \{e_{\theta_i}(T) | \theta_i(T) \in \Omega(\theta)\}$. Consider two invariant level sets, $L_V(m_\rho) := \{e_\rho \in \mathbb{R}^N | : V(e_\rho) \le m_\rho\}$ and $L_V(m_\theta) := \{e_\theta \in \mathbb{R}^N | : V(e_\theta) \le m_\theta\}$. Then

$$\begin{aligned} \rho_i(T) &\le \sqrt{\frac{m_\rho}{N\varepsilon^*}} + \rho_0 = \rho_m \\ \delta\theta_i(T) &= e_{\theta_i}(T) + \frac{2\pi}{N} \le \sqrt{\frac{m_\theta}{N\varepsilon^*}} + \frac{2\pi}{N} = \delta\theta_m \end{aligned}$$

as long as $x_i(0) \in \Omega(x)$ and $\theta_i(T) \in \Omega(\theta)$. One has

$$u_i^* = \begin{bmatrix} -\varepsilon^*(\rho_i - \rho_0) \\ \varepsilon^*\delta\theta_i + \varepsilon^*\eta_\theta \end{bmatrix} \le \begin{bmatrix} \sqrt{\frac{\varepsilon^* m_\rho}{N}} \\ \varepsilon^*\delta\theta_m + \varepsilon^*\eta_\theta \end{bmatrix} \tag{42}$$

with the parameter ε^*, $\|u_i^*\| \le \delta^*$. Moreover, $\|R(\rho_i, \theta_i)\| \le \max\{\rho_m, 1\} = \varpi_\rho$, and $\|x_i\| \le \|r\| + \rho_m$. Then, with Assumption 4, one has

$$\left\| R(\rho_i, \theta_i)u_i^* + Sr - Ax_i \right\| \le \Delta \tag{43}$$

where $\varpi_r = [(\Delta - \delta^*\varpi_\rho - \omega_0\rho_m)/(\kappa_s(\omega_0 + \|S\|))]$.

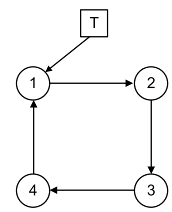

Fig. 3. Network topology. Here, the square and circles denote the target and the agents, respectively, and the arrows represent information transferring connections.

Next, the derivative of $V(e_\rho)$ is calculated, yielding

$$\begin{aligned} \dot{V}(e_\rho) &= \sum_{i=1}^N 2\varepsilon^* e_{\rho_i}\dot{e}_{\rho_i} = \sum_{i=1}^N 2\varepsilon^* e_{\rho_i}(-\varepsilon^* e_{\rho_i}) \\ &= -\sum_{i=1}^N 2\varepsilon^{*2} e_{\rho_i}^2 \le 0 \end{aligned} \tag{44}$$

where "=" holds if and only if $e_{\rho_i} = 0$, i.e., $\rho_i = \rho_0$, which implies that $\lim_{t\to\infty} e_{\rho_i} = 0$ and

$$\lim_{t\to\infty} \|\rho_i\| = \lim_{t\to\infty} \|x_i - r\| = \rho_0.$$

Then, the derivative of e_θ is evaluated, yielding

$$\begin{aligned} \dot{e}_{\theta_i} &= \dot{\theta}_{i+1} - \dot{\theta}_i = \varepsilon^*\left(e_{\theta_{i+1}} - e_{\theta_i}\right) \\ \dot{e}_{\theta_N} &= \varepsilon^*\left(e_{\theta_1} - e_{\theta_N}\right) \end{aligned}$$

which immediately leads to that

$$\begin{aligned} \dot{V}(e_\theta) &= 2\sum_{i=1}^{N-1} e_{\theta_i}\varepsilon^*\left(e_{\theta_{i+1}} - e_{\theta_i}\right) + 2e_{\theta_N}\varepsilon^*\left(e_{\theta_1} - e_{\theta_N}\right) \\ &= -\varepsilon^*\Big[\left(e_{\theta_i}^2 - 2e_{\theta_1}e_{\theta_2} + e_{\theta_2}^2\right) \\ &\quad + \cdots + e_{\theta_N}^2 - 2e_{\theta_N}e_{\theta_1} + e_{\theta_1}^2\Big] \\ &= -\varepsilon^*\left[\sum_{i=1}^{N-1}\left(e_{\theta_i} - e_{\theta_{i+1}}\right)^2 + \left(e_{\theta_N} - e_{\theta_1}\right)^2\right] \le 0 \end{aligned}$$

where = holds if and only if $e_{\theta_1} = e_{\theta_2} = \cdots = e_{\theta_N}$. Moreover, notice that $\sum_{i=1}^N e_{\theta_i} = 0$. One has $e_{\theta_1} = e_{\theta_2} = \cdots = e_{\theta_N} = 0$ if $\dot{V}(e_\theta) = 0$. It follows that:

$$\lim_{t\to\infty} |\theta_2 - \theta_1| = \cdots = \lim_{t\to\infty} |\theta_1 - \theta_N| = 2\pi/N.$$

Consequently, the angular velocities converge to the same value. Therefore, $L_V(m_\theta, m_\rho) = \{\mathrm{col}\{e_\rho, e_\theta\} \in \mathbb{R}^{2N} | e_\rho \in L_V(m_\rho),\ e_\theta \in L_V(m_\theta)\}$ is an invariant set according to the LaSalle invariant theorem. The proof is thus completed. ∎

Remark 6: In Stage 1, the distributed controller (16) is implemented to tune the errors between the agents and the target toward the reference system, such that all the agents will encircle the target. In Stage 2, by delicately adjusting the repulsion between each pair of neighboring agents according to the phase control law (40), all the agents will eventually rotate around the target with evenly distributed phase angles.

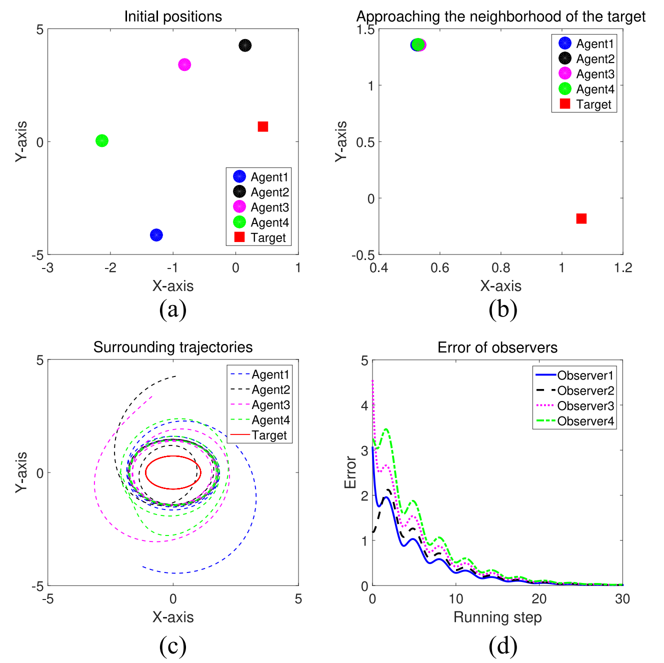

Fig. 4. Simulation results of Stage 1. (a) Initial positions. (b) Approaching the neighborhood of the target. (c) Trajectories of the MAS (7) (dashed lines) and the moving target (solid line). (d) Error e' evolution of the observer (14).

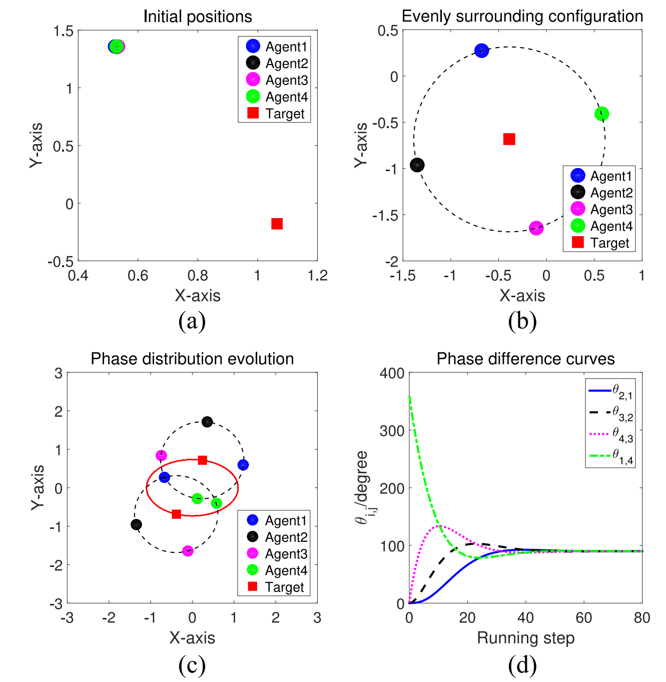

Fig. 5. Simulation results of Stage 2. (a) Initial positions. (b) Evenly surrounding configuration. (c) Two snapshots of the phase distribution evolution. (d) Evolution of the phase differences $\theta_{i,j} := \theta_i - \theta_j$, with $j = 1, 2, \ldots, N$ and $i = j + 1$ with $1 = N + 1$.

IV. Numerical Example

This section presents a numerical case study to verify the effectiveness of the proposed control laws (16) and (40). Consider a MAS consisting of $N = 4$ agents and one target T. Fig. 3 shows the network topology, where the arrows represent the information transferring connections.

The system matrices in (7) and (8) are chosen as

$$A = \begin{bmatrix} 0 & -1 \\ 1 & 0 \end{bmatrix}, \quad S = \begin{bmatrix} 0 & -3/2 \\ 2/3 & 0 \end{bmatrix}$$

where all eigenvalues of S are simple and on the image axis. The observer matrix in (12) is chosen as

$$C_r = \begin{bmatrix} -1 & 0 \\ 0 & -1 \end{bmatrix}.$$

The Laplacian L and the matrix G are as follows:

$$L = \begin{bmatrix} 1 & 0 & 0 & -1 \\ -1 & 1 & 0 & 0 \\ 0 & -1 & 1 & 0 \\ 0 & 0 & -1 & 1 \end{bmatrix}, \quad G = \begin{bmatrix} 0 & 0 & 0 & 0 \\ 0 & 0 & 0 & 0 \\ 0 & 0 & 0 & 0 \\ 0 & 0 & 0 & 0 \end{bmatrix}.$$

The initial state of each agent is chosen from $[5\cos\theta_i, 5\sin\theta_i]^{\mathsf{T}}$, where θ_i is randomly picked from $[0, 2\pi]$

$$x_1(0) = [-1.2628, -4.1371]^{\mathsf{T}}, \; x_2(0) = [0.1472, 4.2650]^{\mathsf{T}}$$
$$x_3(0) = [-0.8140, 3.3997]^{\mathsf{T}}, \; x_4(0) = [-2.1373, 0.0514]^{\mathsf{T}}.$$

The initial state of the target is $r(0) = [0.4322, 0.6732]^{\mathsf{T}}$ and the initial states of observers $\widehat{r}_i$ are

$$\widehat{r}_1(0) = [-2.0729, -1.1527]^{\mathsf{T}}, \; \widehat{r}_2(0) = [1.0697, -0.3529]^{\mathsf{T}}$$
$$\widehat{r}_3(0) = [-2.9341, -2.4857]^{\mathsf{T}}$$
$$\widehat{r}_4(0) = [-1.3359, -2.0524]^{\mathsf{T}}.$$

The matrix $P(\varepsilon)$ in the algebraic Riccati equation is obtained by using standard numerical software, as

$$P(\varepsilon) = \begin{bmatrix} 0.2236 & 0 \\ 0 & 0.2236 \end{bmatrix}$$

with $\varepsilon = 0.05$. The other parameters are set as $\varepsilon^* = 0.1$, $\eta_\theta = 5$, and $\rho_0 = 1$.

By using the proposed distributed target surrounding control laws (16) and (40), results of the numerical simulations are presented in Figs. 4 and 5. Fig. 4(a) and (b) shows the initial positions and convergent positions of the MASs and the target, respectively. Fig. 4(c) demonstrates the system trajectory evolution. Apparently, all the agents move around the target with a certain radius when reaching rendezvous. To verify the state observer (12) for the target, the estimated error between the observer $\widehat{r}$ and the target r is exhibited, which settles down to zero in less than 30 iterations. Fig. 5(b) shows that all the agents are evenly located on the circle centered at the target. Specifically, the phase differences between each pair of neighboring agents converge to $2\pi/N$, as shown in Fig. 5(d). The feasibility of the phase controller (40) is thus verified.

Therefore, the proposed control algorithm (16) and (40) achieves uniform surrounding control for a moving target with input saturation.

V. Experiments

The experiment is performed in our established indoor multi-USV platform (as shown in Fig. 6), which consists of a USV motion capture system, a control server, four 30-cm USVs, and a 3 m $\times$ 4 m pool. Therein, one of the USVs

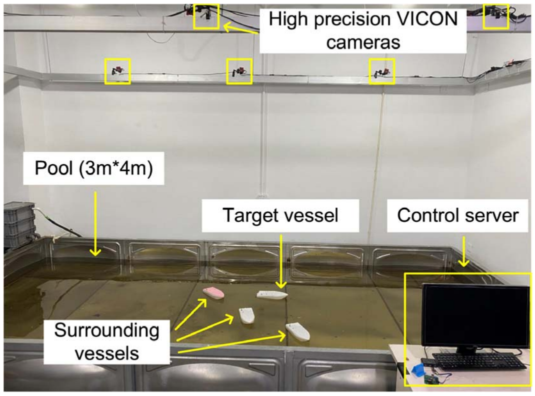

Fig. 6. Established indoor multi-USV platform.

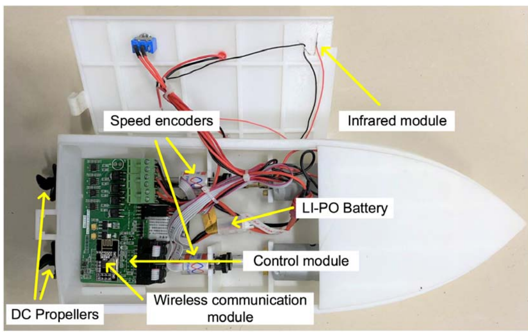

Fig. 7. Configuration of the vessel.

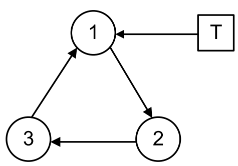

Fig. 8. Intervessel communication network. Here, the square and circles denote the target vessel and the surrounding vessels, respectively.

acts as the moving target, and the other three are agents to fulfill the encirclement task. Every vessel is equipped with two dc propellers, two-speed encoders, a wireless communication module, a control module, an infrared module, and an LI-PO battery (as shown in Fig. 7). The position of each vessel is detected by a motion capture system composed of eight high-precision VICON camera and onboard infrared emitters.

The intervessel communication network is shown in Fig. 8. The initial positions of the agents are set as $p_1 = [-679.3, -135.8]^{\mathrm{T}}$mm, $p_2 = [-829.5, -497.4]^{\mathrm{T}}$mm, and $p_3 = [-1394.9, 245.2]^{\mathrm{T}}$mm. The initial position of the target is set as $p_t = [341.7, -95.0]^{\mathrm{T}}$mm. The desired surrounding radius $\rho_0 = 250$ mm, the other parameters are set as $\varepsilon = 0.05$, $\varepsilon^* = 0.5$, and $\eta_\theta = 5$.

The moving trajectories of the target and the surrounding vessels are all recorded and plotted. The initial positions of the target and surrounding vessels are shown in Fig. 9(a), where the red vessel is the moving target, whereas the black ones are surrounding vessels. Fig. 9(b) shows the completion of Stage 1 (approaching stage). Stage 2 (phase distribution stage) is presented in Fig. 9(c) and the ultimate balanced surrounding formation is shown in Fig. 9(d). Snapshots are given

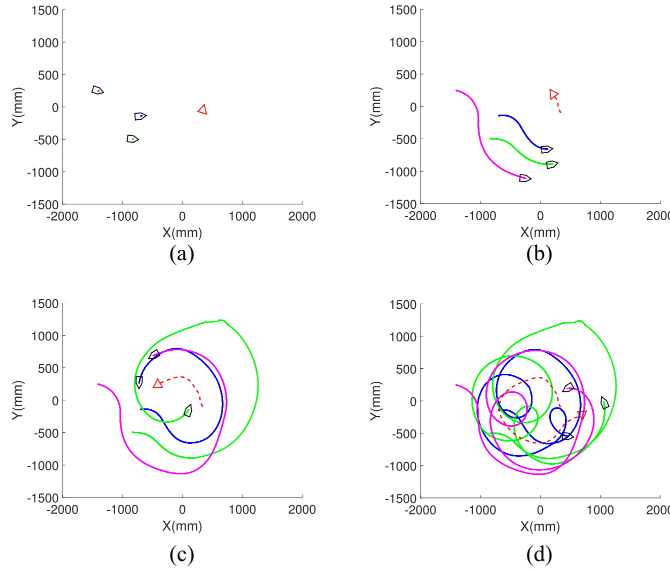

Fig. 9. Experimental performances of the moving target surrounding experiment by multiple USVs. (a) Initial positions distribution. (b) Stage 1 (approaching stage). (c) Stage 2 (phase distribution stage). (d) Balanced surrounding accomplishment.

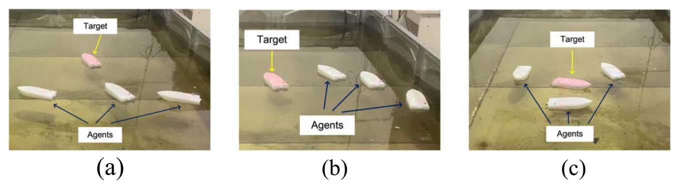

Fig. 10. Three snapshots of the moving target surrounding experiment by multiple USVs. (a) Initial positions distribution. (b) Stage 1 (approaching stage). (c) Balanced surrounding accomplishment.

in Fig. 10, which demonstrates that the desired surrounding formation pattern is gradually achieved.

VI. Conclusion

In this article, the balanced surrounding control problem for a moving target is investigated. A two-stage control algorithm is proposed with the assistance of the algebraic graph theory and the low gain feedback control technique. If all the agents start from a given bounded set, an evenly distributed surrounding configuration can be achieved. The effectiveness of the proposed control algorithm is verified by both numerical simulations and experiments.

References

[1] B. Liu *et al.*, "Collective dynamics and control for multiple unmanned surface vessels," *IEEE Trans. Control Syst. Technol.*, vol. 28, no. 6, pp. 2540–2547, Nov. 2020, doi: 10.1109/TCST.2019.2931524.

[2] Z. Li, W. Yuan, Y. Chen, F. Ke, X. Chu, and C. L. P. Chen, "Neural-dynamic optimization-based model predictive control for tracking and formation of nonholonomic multirobot systems," *IEEE Trans. Neural Netw. Learn. Syst.*, vol. 29, no. 12, pp. 6113–6122, Dec. 2018.

[3] Z. Li, J. Li, S. Zhao, Y. Yuan, Y. Kang, and C. L. P. Chen, "Adaptive neural control of a kinematically redundant exoskeleton robot using brain–machine interfaces," *IEEE Trans. Neural Netw. Learn. Syst.*, vol. 30, no. 12, pp. 3558–3571, Dec. 2019.

[4] Z. Li *et al.*, "Hybrid brain/muscle signals powered wearable walking exoskeleton enhancing motor ability in climbing stairs activity," *IEEE Trans. Med. Robot. Bionics*, vol. 1, no. 4, pp. 218–227, Nov. 2019.

[5] T. Vicsek and A. Zaferis, "Collective motion," *Phys. Rep.*, vol. 517, pp. 71–140, Aug. 2012.

[6] S. B. Meskina, N. Doggaz, M. Khalgui, and Z. Li, "Multiagent framework for smart grids recovery," *IEEE Trans. Syst., Man, Cybern., Syst.*, vol. 47, no. 7, pp. 1284–1300, Jul. 2017.

[7] H.-T. Zhang, Z. Chen, and X. Mo, "Effect of adding edges to consensus networks with directed acyclic graphs," *IEEE Trans. Autom. Control*, vol. 62, no. 9, pp. 4891–4897, Sep. 2017.

[8] Z.-G. Wu, Y. Xu, Y.-J. Pan, P. Shi, and Q. Wang, "Event-triggered pinning control for consensus of multiagent systems with quantized information," *IEEE Trans. Syst., Man, Cybern., Syst.*, vol. 47, no. 11, pp. 1929–1938, Nov. 2018.

[9] H. Meng, H.-T. Zhang, Z. Wang, and G. Chen, "Event-triggered control for semiglobal robust consensus of a class of nonlinear uncertain multiagent systems," *IEEE Trans. Autom. Control*, vol. 65, no. 4, pp. 1683–1690, Apr. 2020.

[10] J. Lunze, "Synchronization of heterogeneous agents," *IEEE Trans. Autom. Control*, vol. 57, no. 11, pp. 2885–2890, Nov. 2012.

[11] W. He, G. Chen, Q.-L. Han, W. Du, J. Cao, and F. Qian, "Multiagent systems on multilayer networks: Synchronization analysis and network design," *IEEE Trans. Syst., Man, Cybern., Syst.*, vol. 47, no. 7, pp. 1655–1667, Jul. 2017.

[12] Y. Liu *et al.*, "Motor-imagery-based teleoperation of a dual-arm robot performing manipulation tasks," *IEEE Trans. Cogn. Develop. Syst.*, vol. 11, no. 3, pp. 414–424, Sep. 2019.

[13] H.-T. Zhang, Z. Cheng, G. Chen, and C. Li, "Model predictive flocking control for second-order multi-agent systems with input constraints," *IEEE Trans. Circuits Syst. I, Reg. Papers*, vol. 62, no. 6, pp. 1599–1606, Jun. 2015.

[14] S. Chen, H. Pei, Q. Lai, and H. Yan, "Multitarget tracking control for coupled heterogeneous inertial agents systems based on flocking behavior," *IEEE Trans. Syst., Man, Cybern., Syst.*, vol. 49, no. 12, pp. 2605–2611, Dec. 2019.

[15] H. Su, X. Wang, and Z. Lin, "Flocking of multi-agents with a virtual leader," *IEEE Trans. Autom. Control*, vol. 54, no. 2, pp. 293–307, Feb. 2009.

[16] Y. Cao, W. Yu, W. Ren, and G. Chen, "An overview of recent progress in the study of distributed multi-agent coordination," *IEEE Trans. Ind. Informat.*, vol. 9, no. 1, pp. 427–438, Feb. 2013.

[17] G. Wen, X. Yu, W. Yu, and J. Lü, "Coordination and control of complex network systems with switching topologies: A survey," *IEEE Trans. Syst., Man, Cybern., Syst.*, early access, Jan. 9, 2020, doi: 10.1109/TSMC.2019.2961753.

[18] Z. Li, J. Li, and Y. Kang, "Adaptive robust coordinated control of multiple mobile manipulators interacting with rigid environments," *Automatica*, vol. 46, pp. 2028–2034, Dec. 2010.

[19] T. H. Kim and T. Sugie, "Cooperative control for target-capturing task based on a cyclic pursuit strategy," *Automatica*, vol. 43, pp. 1426–1431, Aug. 2007.

[20] S. Hara, T. H. Kim, and Y. Hori, "Distributed formation control for target-enclosing operations based on a cyclic pursuit strategy," *IFAC Proc. Vol.*, vol. 41, no. 2, pp. 6602–6607, 2008.

[21] F. Chen, W. Ren, and Y. Cao, "Surrounding control in cooperative agent networks," *Syst. Control Lett.*, vol. 59, pp. 704–712, Nov. 2010.

[22] Y. Lan, G. Yan, and Z. Lin, "Distributed control of cooperative target enclosing based on reachability and invariance analysis," *Syst. Control Lett.*, vol. 59, pp. 381–389, Jul. 2010.

[23] R. Zheng, Y. Liu, and D. Sun, "Enclosing a target by nonholonomic mobile robots with bearing-only measurements," *Automatica*, vol. 53, pp. 400–407, Mar. 2015.

[24] Z. Chen, "A cooperative target-fencing protocol of multiple vehicles," *Automatica*, vol. 107, pp. 591–594, Sep. 2019.

[25] J. Guo, G. Yan, and Z. Lin, "Local control strategy for moving-target-enclosing under dynamically changing network topology," *Syst. Control Lett.*, vol. 59, pp. 654–661, Oct. 2010.

[26] Y. J. Shi, R. Li, and T. T. Wei, "Target-enclosing control for second-order multi-agent systems," *Int. J. Syst. Sci.*, vol. 46, no. 12, pp. 2279–2286, 2015.

[27] Y. J. Shi, R. Li, and K. L. Teo, "Cooperative enclosing control for multiple moving targets by a group of agents," *Int. J. Control*, vol. 88, no. 1, pp. 80–89, 2015.

[28] R. Sharma, M. Kothari, C. N. Taylor, and I. Postlethwaite, "Cooperative target-capturing with inaccurate target information," in *Proc. Amer. Control Conf.*, Baltimore, MD, USA, 2010, pp. 5520–5525.

[29] K. M. Lieberman, G. K. Fricke, and D. P. Garg, "Decentralized control of multi-agent escort formation via morse potential function," in *Proc. ASME 5th Annu. Dyn. Syst. Control Conf. Joint JSME 11th Motion Vib. Conf.*, 2012, pp. 317–324.

[30] P. M. Morse, "Diatomic molecules according to the wave mechanics. II. Vibrational levels," *Phys. Rev.*, vol. 34, p. 57, Jul. 1929.

[31] A. J. Marasco, S. N. Givigi, and C. A. Rabbath, "Model predictive control for the dynamic encirclement of a target," in *Proc. Amer. Control Conf.*, Montreal, QC, Canada, 2012, pp. 2004–2009.

[32] M. Iskandarani, S. N. Givigi, C. A. Rabbath, and A. Beaulieu, "Linear model predictive control for the encirclement of a target using a quadrotor aircraft," in *Proc. 21st Mediterr. Conf. Control Autom.*, Chania, Greece, 2013, pp. 1550–1556.

[33] A. Sharghi, M. Baradarannia, and F. Hashemzadeh, "Adaptive surrounding control for linear multi-agent systems with unknown disturbance," in *Proc. IOP Conf. Mater. Sci. Eng.*, vol. 361, 2018, Art. no. 012024.

[34] A. Franchi, P. Stegagno, and G. Oriolo, "Decentralized multi-robot encirclement of a 3D target with guaranteed collision avoidance," *Auton. Robots*, vol. 40, pp. 245–265, Feb. 2016.

[35] L. Mo, X. Yuan, and Q. Li, "Finite-time rotating target-encirclement motion of multi-agent systems with a leader," *Chin. J. Phys.*, vol. 56, pp. 2265–2274, Oct. 2018.

[36] A. Sharghi, M. Baradarannia, and F. Hashemzadeh, "Finite-time-estimation-based surrounding control for a class of unknown nonlinear multi-agent systems," *Nonlinear Dyn.*, vol. 96, pp. 1795–1804, Mar. 2019.

[37] D. Ma and Y. Sun, "Finite-time circle surrounding control for multi-agent systems," *Int. J. Control Autom. Syst.*, vol. 15, pp. 1536–1543, Jun. 2017.

[38] L. Brinón-Arranz, A. Seuret, and C. Canudas de Wit, "Cooperative control design for time-varying formations of multi-agent systems," *IEEE Trans. Autom. Control*, vol. 59, no. 8, pp. 2283–2288, Aug. 2014.

[39] X. Yu and L. Liu, "Cooperative control for moving-target circular formation of nonholonomic vehicles," *IEEE Trans. Autom. Control*, vol. 62, no. 7, pp. 3448–3454, Jul. 2017.

[40] X. Yu, J. Ma, N. Ding, and A. Zhang, "Cooperative target enclosing control of multiple mobile robots subject to input disturbances," *IEEE Trans. Syst., Man, Cybern., Syst.*, early access, Jul. 24, 2019, doi: 10.1109/TSMC.2019.2926534.

[41] X. Peng, K. Guo, X. Li, and Z. Geng, "Cooperative moving-target enclosing control for multiple nonholonomic vehicles using feedback linearization approach," *IEEE Trans. Syst., Man, Cybern., Syst.*, early access, Oct. 11, 2019, doi: 10.1109/TSMC.2019.2944539.

[42] Z. Lin, "Control design in the presence of actuator saturation: From individual systems to multi-agent systems," *Sci. China Inf. Sci.*, vol. 62, no. 2, 2019, Art. no. 026201.

[43] L. M. Chen, Y. Y. Lv, C. J. Li, and G. F. Ma, "Cooperatively surrounding control for multiple Euler–Lagrange systems subjected to uncertain dynamics and input constraints," *Chin. Phys. B*, vol. 25, Oct. 2016, Art. no. 128701.

[44] T. Zhang, J. Ling, and L. Mo, "Distributed finite-time rotating encirclement control of multiagent systems with nonconvex input constraints," *IEEE Access*, vol. 7, pp. 102477–102486, 2019.

[45] H. J. Sussmann, E. D. Sontag, and Y. Yang, "A general result on the stabilization of linear systems using bounded controls," *IEEE Trans. Autom. Control*, vol. 39, no. 12, pp. 2411–2425, Dec. 1994.

[46] Z. Lin, *Low Gain Feedback*. London, U.K.: Springer, 1999.

[47] Y. Su and J. Huang, "Cooperative output regulation of linear multi-agent systems," *IEEE Trans. Autom. Control*, vol. 57, no. 4, pp. 1062–1066, Apr. 2012.

[48] Z. Li, Z. Duan, G. Cheng, and L. Huang, "Consensus of multiagent systems and synchronization of complex networks: A unified viewpoint," *IEEE Trans. Circuits Syst. I, Reg. Paper*, vol. 57, no. 1, pp. 213–224, Jan. 2010.

[49] L. Zhu, Z. Chen, and R. H. Middleton, "A general framework for robust output synchronization of heterogeneous nonlinear networked systems," *IEEE Trans. Autom. Control*, vol. 61, no. 8, pp. 2092–2107, Aug. 2016.

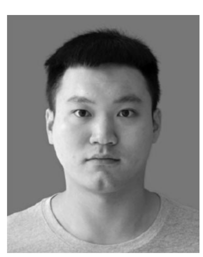

Bowen Xu (Member, IEEE) received the B.E. degree in automation from Xidian University, Xi'an, China, in 2016. He is currently pursuing the Ph.D. degree with the School of Artificial Intelligence and Automation, Huazhong University of Science and Technology, Wuhan, China.

His research interests include multiagent systems and formation control.

Mr. Xu was a recipient of the 2017 Outstanding Reviewer Award of *Asian Journal of Control*.

Hai-Tao Zhang (Senior Member, IEEE) received the B.E. and Ph.D. degrees from the University of Science and Technology of China, Hefei, China, in 2000 and 2005, respectively.

In 2007, he was a Postdoctoral Researcher with the University of Cambridge, Cambridge, U.K. Since 2005, he has been with the Huazhong University of Science and Technology, Wuhan, China, where he was an Associate Professor from 2005 to 2010, and has been a Full Professor since 2010. He is a Cheung Kong Young Scholar. His research interests include swarming intelligence, model predictive control, and unmanned system cooperation control.

Prof. Zhang is/was an Associate Editor of IEEE TRANSACTIONS ON SYSTEMS, MAN, AND CYBERNETICS: SYSTEMS, IEEE TRANSACTIONS ON CIRCUITS AND SYSTEMS—PART II: EXPRESS BRIEFS, *Asian Journal of Control*, IEEE Conference on Decision and Control, and American Control Conference.

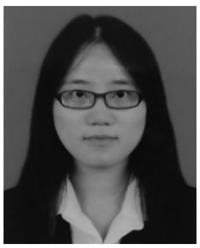

Haofei Meng received the B.Eng. degree from the Wuhan University of Technology, Wuhan, China, in 2010, the M.Eng. degree from the University of Science and Technology of China, Hefei, China, in 2013, and the Ph.D. degree from the University of Newcastle, Callaghan, NSW, Australia, in 2017.

She has been working as a Postdoctoral Fellow with the Huazhong University of Science and Technology since 2018. Her research interests include multiagent systems, time-delay systems, and switched systems.

Binbin Hu received the B.E. degree in electrical engineering and automation from Jiangnan University, Wuxi, China, in 2017. He is currently pursuing the Ph.D. degree in control science and technology with the Huazhong University of Science and Technology, Wuhan, China.

His research interests include multiagent systems and control of unmanned surface vehicles.

Duxin Chen (Member, IEEE) received the B.Sc. and Ph.D. degrees in control science and engineering from the Huazhong University of Science and Technology, Wuhan, China, in 2013 and 2018, respectively.

He is currently a Lecturer with the School of Mathematics, Southeast University, Nanjing, China. His research interests include complex networks, distributed control, and intelligent transportation system.

Dr. Chen serves as an active reviewer for tens of international journals.

Guanrong Chen (Life Fellow, IEEE) received the M.Sc. degree in computer science from Sun Yat-sen University, Guangzhou, China, in 1981, and the Ph.D. degree in applied mathematics from Texas A&M University, College Station, TX, USA, in 1987.

He was a tenured Full Professor with the University of Houston, Houston, TX, USA. He has been a Chair Professor and the Founding Director of the Centre for Chaos and Complex Networks, City University of Hong Kong, Hong Kong, since 2000.

Prof. Chen received the State Natural Science Award of China in 2008, 2012, and 2016, respectively. He was awarded the 2011 Euler Gold Medal, Russia, and conferred Honorary Doctorates by the Saint Petersburg State University, Russia, in 2011 and by the University of Le Havre, Normandy, France, in 2014. He has been a Highly Cited Researcher in Engineering according to Thomson Reuters since 2009. He is a member of the Academy of Europe and a Fellow of the World Academy of Sciences.